Neutron lifetime from a new evaluation of ultracold neutron storage experiments

A. P. Serebrov* and A. K. Fomin
Petersburg Nuclear Physics Institute, Russian Academy of Sciences, Gatchina, RU-188300 Leningrad, Russia
(Received 2 June 2010; published 9 September 2010)

An analysis of data on measurements of neutron lifetime is presented. The new most accurate result of the measurement of neutron lifetime [Phys. Lett. B **605**, 72 (2005)] 878.5 ± 0.8 s, differs from the world average value [Phys. Lett. B **667**, 1 (2008)] 885.7 ± 0.8 s, by 6.5 standard deviations. In this connection an analysis and Monte Carlo simulation of experiments [Phys. Lett. B **483**, 15 (2000)] and [Phys. Rev. Lett. **63**, 593 (1989)] is carried out. Systematic errors of about -6 s are found in each of the experiments. A summary table of neutron lifetime measurements after corrections and additions is given. A new world average value for neutron lifetime, 879.9 ± 0.9 s, is presented.

DOI: 10.1103/PhysRevC.82.035501 PACS number(s): 13.30.Ce, 14.20.Dh

I. INTRODUCTION

A recent neutron lifetime experiment [1] has provided the value 878.5 ± 0.8 s. It differs by 6.5 standard deviations from the world average value of 885.7 ± 0.8 s quoted by the particle data group (PDG) in 2006 [2]. The experiment employed a gravitational trap with a low-temperature fluorinated oil (Fomblin) coating, which provides several advantages with respect to previous experiments. First, the small loss factor of only 2×10^{-6} per collision of ultracold neutrons (UCNs) with trap walls results in the low loss probability of only 1% of the probability of neutron β decay. Therefore the measurement of neutron lifetime was almost direct; the extrapolation from the best storage time to the neutron lifetime was only 5 s. Under these conditions it is practically impossible to obtain a systematic error of about 7 s. The quoted systematical error of the experimental result [1] was 0.3 s.

In the determination of the world average value of neutron lifetime there is a rather dramatic situation. On the one hand, the new value of neutron lifetime from Ref. [1] cannot be included in the world average value because of the big difference in the results. On the other hand, until this major disagreement is understood, the present world average value for the neutron lifetime must be suspect. So the situation on the PDG page devoted to the neutron lifetime is formulated [2] in view of this controversy.

The only way out of the present situation is to carry out new, more precise experiments. More detailed analysis of the previous experiments and a search for possible systematic error are also reasonable.

The column "till 2007" in Table I and Fig. 1 show the dynamics of developing events. Before measurements [1] using the Gravitrap installation were carried out, the world average neutron lifetime was mainly determined by the result in Ref. [6]. At that time the consistent world average value of 885.7 ± 0.8 s was obtained. The determination of a new precise measurement of neutron lifetime in 2004 led to the aforementioned controversy. It became more obvious in 2007 after measurements of neutron lifetime with the UCN magnetic trap were obtained [4]. It is easy to see that the experiment in Ref. [6] is one of the most precise experiments in the column "till 2007" in Table I. Not only does it make the main contribution to the world average value obtained until 2004, but it also makes the main contribution to the discrepancy between the results of earlier and those of new measurements.

We cannot find by any means an error of 7 s in our measurements [1] where extrapolation of UCN storage time to neutron lifetime is only 5 s. Therefore we have examined the analysis of the experiment [6] where the extrapolation is 100–120 s, and at the same time it is affirmed that it is done with a systematic error of 0.4 s. It is this point that causes obvious doubts. A detailed analysis of the experiment [6] performed by means of Monte Carlo (MC) simulation is made here in Sec. II. In Sec. III an analysis of the MAMBO I experiment [13] is given. In this experiment the effect of quasielastic UCN scattering on Fomblin oil was taken into account. In Sec. IV an analysis of the summary table for the neutron lifetime measurements after corrections and additions is made. A new world average value for the neutron lifetime is also presented.

II. A DETAILED ANALYSIS OF THE EXPERIMENT IN REF. [6]

A. Scheme and method of the experiment [6]

Here we reproduce a short description of the experiment [6] using mainly the text of that article. The setup is shown in Fig. 2. The storage vessel, (7) and (8), is composed of two coaxial horizontal cylinders made of 2-mm-thick aluminium. The cylinder walls were coated with a thin layer of Fomblin oil, which has very low UCN losses. To maintain this oil layer on the surface, the cylinder walls were first coated with a layer of Fomblin grease about 0.2 mm thick.

The inner cylinder (7) was 33 cm in diameter and 90 cm long, while the dimensions of the outer cylinder (8) were larger by a gap of 2.5 cm. Shutter 6 connects the inner cylinder to the intermediate chamber, which has connections (i) to the neutron guide (1) of the TGV UCN source by the entrance shutter and (ii) to the UCN detector (3) by shutter 2. Shutter 13 connects the inner cylinder to the volume of the annular gap between the two cylinders.

*serebrov@pnpi.spb.ru

TABLE I. Experimental results for neutron lifetime.

Author(s), year [ref. no.]	τ_n (s) till 2007	τ_n (s), corrections and additions
Arzumanov *et al.*, 2009 [3]		881.5 ± 2.5
Ezhov *et al.*, 2007 [4]	878.2 ± 1.9	
Serebrov *et al.*, 2005 [1]	878.5 ± 0.7 ± 0.3	
Dewey *et al.*, 2003 [5]	886.3 ± 1.2 ± 3.2	
Arzumanov *et al.*, 2000 [6], Fomin and Serebrov, 2010 [7]	885.4 ± 0.9 ± 0.4	879.9 ± 0.9 ± 2.4
Pichlmaier *et al.*, 2000 [8]		881.0 ± 3
Byrne *et al.*, 1996 [9]	889.2 ± 3.0 ± 3.8	
Mampe *et al.*, 1993 [10]	882.6 ± 2.7	
Nesvizhevski *et al.*, 1992 [11]	888.4 ± 3.1 ± 1.1	Removed
Byrne *et al.*, 1990 [12]	893.6 ± 3.8 ± 3.7	
Mampe *et al.*, 1989 [13], Serebrov and Fomin, 2009 [14]	887.6 ± 3.0	881.6 ± 3.0
Kharitonov *et al.,* 1989 [15]	872 ± 8	
Kossakowski *et al.,* 1989 [16]	878 ± 27 ± 14	
Paul *et al.*, 1989 [17]	877 ± 10	
Spivac *et al.*, 1988 [18]	891 ± 9	
Last *et al.*, 1988 [19]	876 ± 10 ± 19	
Arnold *et al.*, 1987 [20]	870 ± 17	
Kosvintsev *et al.*, 1986 [21]	903 ± 13	
Byrne *et al.*, 1980 [22]	937 ± 18	
Bondarenko *et al.*, 1978 [23]	881 ± 8	
Christensen *et al.*, 1972 [24]	918 ± 14	

The inner cylinder had a long slit (2a) of a special form (see Fig. 2) along the cylinder surface. The edges of the slit were dipped into a Fomblin oil puddle (1a) with level 12 when the slit was situated at the bottom position during storage. The construction allowed rotation of the cylinders in common about the horizontal axis without a vacuum break to refresh the oil layers on the cylinder walls.

The storage vessel was placed inside the vacuum housing (11). The vessel volume was hermetically sealed from the housing. The housing was formed by two coaxial cylinders of stainless steel. The outer surface of the inner cylinder had a serpent tube (9) to cool the bottles. The cooling system stabilized the bottle temperature, which could be set in the range of +20°C to −26°C.

The setup was surrounded by thermal neutron detectors comprising a set of 24 counters of the SNM-57 type (10), each counter being a ^{3}He-filled tube of 3 cm in diameter and 100 cm long. The UCN detector was a ^{3}He-loaded proportional counter (3) with an Al entrance window 100 μm thick. The whole installation was placed inside a shield (5) of 1-mm-thick Cd and a shield (4) of 16-cm-thick boron polyethylene. The construction permits storage of UCNs either in the inner cylinder or in the annular space between the inner and the outer cylinder, thereby changing the UCN loss rate by a factor of about 5 without breaking the vacuum.

The experiment was carried out using the following sequence of procedures.

(i) Filling. The chosen vessel, annular or central, was filled for 200 s. For filling only the central vessel, shutter 13 was closed. For the annular vessel, shutter 13 was open and the UCN was removed from the central vessel in the following step.

(ii) Cleaning. The trapped neutron spectrum in the storage vessel was given time for cleaing during $t_{\rm cl}$ (200 to 1000 s). This procedure was necessary as the UCN source provided a rather broad neutron spectrum. During the cleaning time $t_{\rm cl}$, UCNs with a velocity exceeding the limiting velocity of Fomblin escaped from the vessel. When the annular vessel was chosen, shutter 6 and the shutter to the UCN detector were opened during $t_{\rm cl}$ to empty the central vessel.

(iii) Emptying. UCNs were emptied to the detector from the chosen vessel and counted for 200 s, yielding the initial quantities N_i and $n_i(t)$, where $n_i(t)$ denotes the counting rate in the UCN detector during the emptying time t, and N_i the integral over $n_i(t)$. Upon emptying of the inner vessel both its shutters were opened to make the emptying conditions more equal for the two vessels.

(iv) Steps 1 and 2 were repeated to fill the chosen vessel and to clean the UCN spectrum before the storage period. Owing to the stable intensity of the UCN source, the initial conditions were essentially identical.

(v) Storing. After the cleaning time, UCNs were further stored in the chosen vessel for time T and inelastically scattered and leaked neutrons were counted during that interval in the thermal neutron and UCN detector, respectively.

(vi) The final UCN quantities N_f and $n_f(t)$ were determined by counting for 200 s (same procedure as step iii).

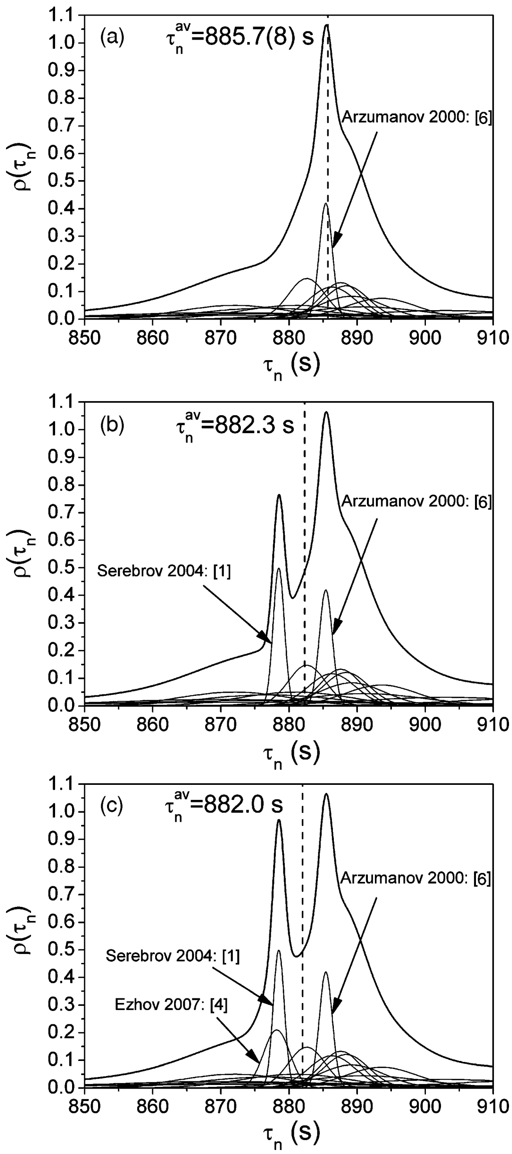

FIG. 1. Progress of neutron lifetime measurements. (a) Before Gravitrap measurement in 2003; (b) after Gravitrap measurement in 2004; (c) after magnetic trap measurement in 2007.

(vii) The background of the detectors was measured during 150 s after all UCNs had left the vessel.

All these procedures are shown in Fig. 3.The basic idea of the experimental method for a monoenergetic UCN spectrum is the following. The number of neutrons $N(t)$ in the trap changes exponentially during the storage time, that is, $N(t) = N_0 e^{-\lambda t}$. The value λ is the total probability per unit time for the disappearance of UCN owing to both β decay and losses during UCN-wall collisions. In turn, losses are equal to the sum of the inelastic scattering rate constant λ_{ie} and that for neutron capture at the wall, λ_{cap}:

$$\lambda = \lambda_{\text{n}} + \lambda_{\text{loss}} = \lambda_{\text{n}} + \lambda_{\text{ie}} + \lambda_{\text{cap}}. \tag{1}$$

The ratio $\lambda_{\text{cap}}/\lambda_{\text{ie}}$ is to a good approximation equal to the ratio of the UCN capture and inelastic scattering cross sections for the material of the wall surface, as both values are proportional

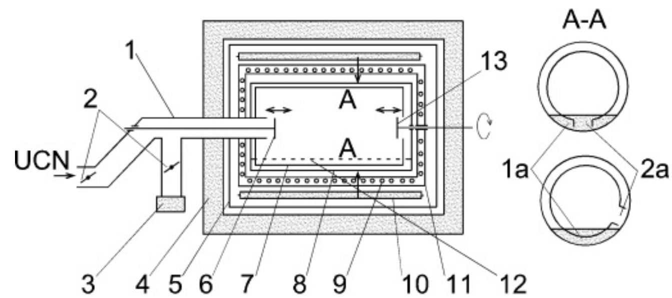

FIG. 2. Scheme of the experimental setup. 1, UCN guide; 2, shutters; 3, UCN detector; 4, polyethylene shielding; 5, cadmium housing; 6, entrance shutter of inner vessel; 7, inner storage vessel; 8, outer storage vessel; 9, cooling coil; 10, thermal neutron detector; 11, vacuum housing; 12, oil puddle; 13, entrance shutter of gap vessel; 1a, oil puddle; 2a, slit.

to the wall reflection rate of UCN in the trap. Hence $\sigma_{\text{cap}}/\sigma_{\text{ie}}$ and the value

$$a = \lambda_{\text{loss}}/\lambda_{\text{ie}} = 1 + \lambda_{\text{cap}}/\lambda_{\text{ie}} = 1 + \sigma_{\text{cap}}/\sigma_{\text{ie}} \tag{2}$$

are constant for the given conditions, that is, the same wall material and temperature. During storage the upscattered neutrons are recorded with an efficiency ε_{th} in the thermal neutron detector surrounding the storage trap. The corresponding counting rate is given by

$$j = \varepsilon_{\text{th}}\lambda_{\text{ie}}N(t). \tag{3}$$

Hence the total counts in the time interval T are equal to

$$J = \varepsilon_{\text{th}}\lambda_{\text{ie}}(N_0 - N_T)/\lambda. \tag{4}$$

Here N_0 and N_T are the UCN populations in the trap at the beginning and the end of the storage time T, respectively. The UCNs themselves are measured with an efficiency ε such that the UCNs detected at the beginning (normalization measurement) and the end of the storage time are equal to $N_i = \varepsilon N_0$ and $N_f = \varepsilon N_T$, respectively. We then have

$$\lambda_{\text{ie}} = \frac{J\lambda}{N_i - N_f}\frac{\varepsilon}{\varepsilon_{\text{th}}}, \tag{5}$$

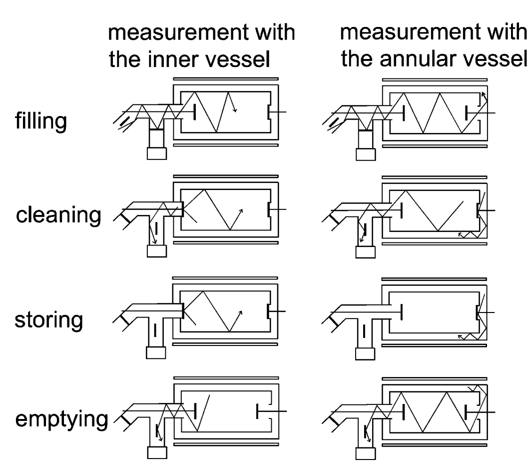

FIG. 3. Experimental procedures.

$$\lambda = \frac{1}{T}\ln(N_i/N_f). \tag{6}$$

The experiment is repeated with different value for the wall loss rates. The ratio of the two corresponding λ values are built following Eq. (1) and including Eq. (2) with a constant value a. Thus λ_n is given by

$$\lambda_n = \frac{\xi\lambda^{(1)} - \lambda^{(2)}}{\xi - 1}, \tag{7}$$

where

$$\xi = \lambda_{ie}^{(2)}/\lambda_{ie}^{(1)}. \tag{8}$$

The indices refer to the two measurements with different λ_{loss} values. Equations (7) and (8) then contain only the directly measured quantities J, N_i, and N_f following Eqs. (5) and (6) because the efficiencies of the neutron detection cancel. The value for λ_{loss} can be varied by changing the ratio of the surface to the volume of the bottle and hence the reflection rate with the walls. To keep the value a constant the (monoenergetic) energy of the UCN and the specification of the wall (temperature, type of wall, etc.) must be the same. A description of this method for a broad UCN spectrum and more experimental details are given in Ref. [6].

B. Analysis and Monte Carlo simulation of the experiment in Ref. [6]

Processing of results of a method in Ref. [6] for extrapolation to the neutron lifetime is presented by Eqs. (7) and (8). For descriptive reasons [Fig. 4(a)] it is possible to suggest a graphic solution, using Eqs. (1) and (2).

From Eqs. (1) and (2) we can write

$$\lambda = \lambda_n + a\lambda_{ie}. \tag{9}$$

Accordingly, for two measurements in different geometry,

$$\lambda^{(1)} = \lambda_n + a\lambda_{ie}^{(1)}, \tag{10}$$

$$\lambda^{(2)} = \lambda_n + a\lambda_{ie}^{(2)}. \tag{11}$$

Excluding a from the system of equations,

$$\lambda_n = \frac{\lambda^{(1)}\lambda_{ie}^{(2)} - \lambda^{(2)}\lambda_{ie}^{(1)}}{\lambda_{ie}^{(2)} - \lambda_{ie}^{(1)}} = \frac{\xi\lambda^{(1)} - \lambda^{(2)}}{\xi - 1}, \tag{12}$$

where $\xi = \lambda_{ie}^{(2)}/\lambda_{ie}^{(1)}$; that is, we derive Eq. (7) of Ref. [6].

It is quite obvious that for the absence of systematics in the method of Ref. [6], it is necessary to have full equivalence of parameters λ and λ_{ie} for two different vessels. We consider possible distinctions for λ and λ_{ie} that arise upon changing the geometry of the experiment.

MC simulation of the experiment in Ref. [6] was performed using a code capable of taking gravity into account. The code was written by A. K. Fomin especially for simulations with UCNs [25]. This code starts with an initial distribution of neutrons and calculates the track of each particle analytically until it reaches a material boundary. For each wall collision the loss and reflection probabilities are calculated, resulting in a new direction for calculation of the trajectory until the next boundary is reached. The code uses specula and diffusion reflections with walls. This code

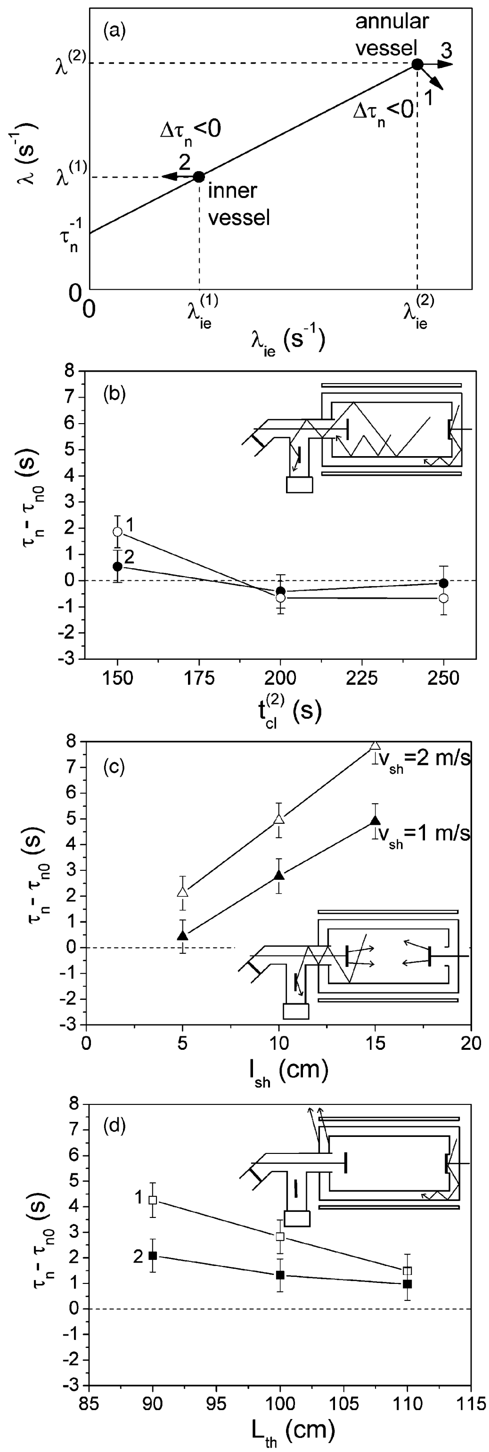

FIG. 4. (a) Diagram showing influence of various effects for measured value of neutron lifetime. (b) Correction of neutron lifetime owing to the effect of incomplete emptying of the inner vessel during cleaning while working with the annular vessel: simulations for neutron guide length in front of the detector of 0.8 m (curve 1) and 1 m (curve 2). (c) Correction of neutron lifetime owing to the effect of heating of neutrons by the shutters. (d) Correction of neutron lifetime owing to the effect of unequal thermal neutron detection efficiencies for different vessels: simulations without capture and scattering in materials (curve 1) and with capture and scattering in materials (curve 2).

was tested with the GEANT4 code adapted to include the influence of gravity on neutrons [26]. Also, its benchmark tests with experimental data are shown in our work in Refs. [1] and [14].

The geometry of setup and time intervals was chosen to be the same as in the experiment. After each simulation we have values of N_i, N_f, J, $j(t)$, and $n(t)$. We evaluate the data obtained in the same way as in the experiment. In all our simulations the neutron lifetime was fixed to a definite value. Repeating the experimental procedure we obtain the extrapolated neutron lifetime values, and comparing them with the initial one we get the corrections to the experimental result.

The percentage values of diffusion reflections by walls were set to reproduce an experimental emptying process, that is, the time dependence of the UCN detector count in the course of registration. It is the most detailed information given in Ref. [6]. Neutron reflection by walls was approximated by 50% specular and 50% diffusion reflections for the inner and annular vessels. These factors seem reasonable, as the surface of vessels was covered by a layer of Fomblin grease before being covered with Fomblin oil. Neutron reflection by walls was approximated by 90% specular and 10% diffusion reflections for the neutron guides. These correspond to the quality of electropolished neutron guides.

MC simulation was done for the temperature −26°C because most of the experimental data were obtained at this temperature. We studied three effects in MC simulations: (1) incomplete emptying of the inner vessel during cleaning while working with the annular vessel, (2) heating of neutrons by shutters, and (3) unequal thermal neutron detection efficiencies for different vessels.

1. *Effect of incomplete emptying of the inner vessel during cleaning while working with the annular vessel*

One can see from Fig. 3 that the process of UCN emptying into the detector after being held in the inner and annular vessels is different. Emptying after holding in the inner vessel occurs directly into the detector through the neutron guide system. However, after holding in the annular vessel, neutrons first pass through the inner vessel. The authors of Ref. [6] tried to make the conditions of emptying more identical, so upon emptying the inner vessel both its shutters were opened to make the emptying conditions more equal for the two vessels. The question arises how perfect emptying of the inner vessel will be obtained before opening of shutter 13 to empty the annular vessel after cleaning. For estimation of the possible systematic error in this process, we have done an MC simulation of the process taking into account the geometry from Ref. [6].

Shutter 6 and the shutter of the UCN detector are opened during $t_{\rm cl}$ when we work with the annular vessel. It is necessary to empty the inner vessel of UCNs during holding in the annular vessel. If this time is not enough for the inner vessel, there are still neutrons that are added to neutrons from the annular vessel during its emptying. This gives a higher value of N_i and, correspondingly, a higher value of λ and lower value of $\lambda_{\rm ie}$ for the annular vessel:

$$\lambda_{\rm ie} = \frac{J\lambda}{(N_i + \Delta N_i) - N_f}\frac{\varepsilon}{\varepsilon_{\rm th}}, \quad (13)$$

$$\lambda = \frac{1}{T}\ln((N_i + \Delta N_i)/N_f), \quad (14)$$

where ΔN_i is the number of UCNs in the inner vessel after cleaning in the annular vessel. Arrow 1 in Fig. 4(a) shows the direction of the changed position of the point for the annular vessel after correction. It gives a negative correction for the measured value of neutron lifetime. The values of $t_{\rm cl}$ for MC simulation are taken from Table 1 in Ref. [6]. The results of extrapolations to neutron lifetime are shown in Fig. 4(b) for different $t_{\rm cl}$ values and different neutron guide lengths in front of the detector, which have not been strictly defined in the experimental geometry data. From the simulation results it is possible to draw the conclusion that the effect of incomplete emptying has not revealed, although the uncertainty of an estimation of this process is at the level of 1 s.

2. *Effect of heating of neutrons by shutters*

The following nonequivalence of measurements for different vessels is observed at emptying. Before release of neutrons into the detector, shutters 6 and 13 are open. At shutter movement in volume of UCNs there is either heating or cooling of UCNs, depending on the direction of movement of the shutter in relation to the UCN gas. In the case of emptying from the inner vessel, shutters move into a vessel with UCNs. There is mainly heating of UCNs. In the case of emptying from the annular vessel, there is mainly UCN cooling, as the shutter escapes UCN flux. It is necessary to note that this effect was observed experimentally. The peaks of heated neutrons are visible in the graphs of the emptying process (Fig. 5) presented in Refs. [27] and [28]. Unfortunately, the effect has not been considered. It is discussed neither in Ref. [6] nor in detailed work on this experiment [28]. These peaks are connected with UCN heating by shutters and are present only in the case of emptying from the inner vessel. Unfortunately, it is obviously

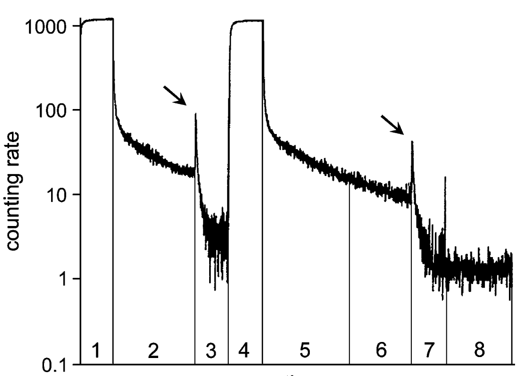

FIG. 5. Thermal neutron detector count for the inner vessel during (1) filling, (2) cleaning, (3) emptying, (4) filling, (5) cleaning, (6) storing, (7) emptying, and (8) background. Effects of heating of neutrons by the shutters are shown by arrows.

not possible to make a numerical estimation from the graphs. Therefore the given process was simulated.

When we work with the inner vessel, shutters 6 and 13 heat the trapped neutron spectrum after holding. Some portion of UCNs is lost owing to this process. This gives a lower value of $(N_i - N_f)$ and a correspondingly higher value of λ_{ie} for the inner vessel:

$$\lambda_{\text{ie}} = \frac{J\lambda}{(N_i - N_f)(1-\delta)} \frac{\varepsilon}{\varepsilon_{\text{th}}}, \tag{15}$$

$$\lambda = \frac{1}{T} \ln \frac{N_i(1-\delta)}{N_f(1-\delta)}, \tag{16}$$

where δ is the portion of neutrons heated by the shutters. Calculations were done with shutter velocities (v_{sh}) of 1 and 2 m/s; the shutter course (l_{sh}) of 5, 10, and 15 cm. Arrow 2 in Fig. 4(a) shows the direction of a changed point position for the inner vessel after correction. It gives a negative correction for the measured value of neutron lifetime. The results of this simulation are shown in Fig. 4(c). The correction for the effect of UCN heating by shutters is −2.8 s for a shutter velocity of 1 m/s and a shutter course of 10 cm. As there are no detailed data on the shutters, we cannot estimate the uncertainty of this effect to better than 2 s. Thus this correction is −2.8 s with an uncertainty of initial data of 2 s.

3. *Effect of unequal thermal neutron detection efficiencies for different vessels*

Another obvious nonequivalence of measurements for different vessels is observed at thermal neutron detection. The issue is that counters of thermal neutrons do not cover the entire external surface of the installation. They are absent at the installation end faces. For this reason, processes of inelastic scattering occurring at the end faces of traps are registered with a geometrical efficiency of about 50%. When neutrons are stored in the inner volume we have two end faces (on the left and the right). But when neutrons are stored in the annular vessel there are four end faces (two on the left and two on the right). In addition, the annular vessel is longer than the inner vessel and its end faces are more forward. Unfortunately the value of this effect in Ref. [28] is underestimated and wrongly considered with an opposite sign. For estimation of the nonequivalence effect in thermal neutrons, simulation of the detection process has also been made.

The thermal detector efficiency is lower for the annular vessel because of the four end faces. It gives a lower value of J and a correspondingly lower value of λ_{ie} for the annular vessel:

$$\lambda_{\text{ie}} = \frac{(J - \Delta J)\lambda}{(N_i - N_f)} \frac{\varepsilon}{\varepsilon_{\text{th}}}, \tag{17}$$

where ΔJ is the number of undetected thermal neutrons for measurement with the annular vessel. We used mean values for the capture and scattering cross sections of materials of the setup from tables [29]. The simulation was done for thermal neutron detector lengths (L_{th}) of 90, 100, and 110 cm. Arrow 3 in Fig. 4(a) shows the direction of the changed point position for the annular vessel after correction. It gives a negative correction for the measured value of neutron lifetime. The results of this simulation are shown in Fig. 4(d).

TABLE II. Monte Carlo correction of the neutron lifetime result of the experiment in Ref. [6].

	Correction (s)	Uncertainty (s)
Incomplete emptying of inner vessel during cleaning while working with annular vessel	0	1
Effect of heating of neutrons by shutters	−2.8	2
Effect of unequal thermal neutron detection efficiencies for different vessels	−2.1	1
Effect of unequal thermal neutron detection efficiencies for different vessels (correction in experiment is +0.6 s)	−0.6	
Total	−5.5	2.4

Geometrically the length of the detector is 100 cm, however, its working area apparently does not exceed 90 cm because of edge effects where devices for fastening of a thread are located. We choose the result of calculation of the working length of the detector of 90 cm and for the case of capture and scattering of neutrons in an installation material. In this section we note that in Ref. [28] the effect of nonequivalence was calculated, but the correction (+0.6 s) appeared to be underestimated and to have the wrong sign. Therefore we must correct this error. Thus, the correction of the effect of unequal thermal neutron detection efficiencies for different vessels is −2.1 s with an uncertainty in the initial data of 1 s.

Figure 4(a) shows that each effect gives a negative correction for the measured value of neutron lifetime. Table II is the summary table of corrections. We assume that after taking MC correction and uncertainty into account, the result in Ref. [6] for neutron lifetime would be $879.9 \pm 0.9_{\text{stat}} \pm 2.4_{\text{syst}}$ s. The resulting corrected value for the neutron lifetime is in agreement with the result 878.5 ± 0.8 s in Ref. [1].

III. A DETAILED ANALYSIS OF THE MAMBO I EXPERIMENT [13]

A. Scheme and method of the experiment [13]

Here we reproduce a short description of the experiment in Ref. [13]. The setup is shown in Fig. 6. The UCN storage volume is a rectangular box, with a constant height of 30 cm and width of 40 cm but a variable length $x < 55$ cm. The side walls and roof of the box are made of 5-mm float-glass plates. The oil spray head is mounted on the metal base plate and the assembly is immersed in a 1-mm-deep lake of oil. The movable rear wall, composed of two glass plates with a 1-mm oil-filled gap in between, has 0.1 mm of play with respect to the neighboring walls, except for the base plate, where it dips into the oil. The surface of the rear wall was covered with 2-mm-deep and 2-mm-wide sinusoidal corrugations. For half the surface the wave crests were horizontal; for the other half, vertical. Within a few seconds this arrangement transforms the forward-directed incoming neutron flux into the isotropic distribution essential for the validity of the mean-free-path formula $\lambda = 4V/S$. The UCN inlet and outlet shutters situated

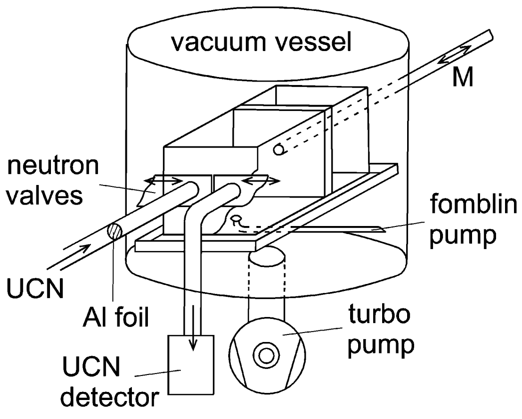

FIG. 6. Sketch of the MAMBO I apparatus.

8 cm above floor level are sliding glass plates with 65-mm holes matching holes in the front wall (Fig. 6). More experimental details are given in Ref. [13].

The main idea of the experiment was to deduce the neutron lifetime from an extrapolation, by variation of the mean free path of UCNs between wall collisions:

$$\tau_{st}^{-1} = \tau_n^{-1} + \mu(\mathrm{v})\nu(\mathrm{v}) = \tau_n^{-1} + \mu(\mathrm{v})\mathrm{v}/\lambda, \qquad (18)$$

where τ_{st}^{-1} is the inversed storage time constant, $\mu(\mathrm{v})$ is the neutron velocity-dependent UCN loss factor per collision, $\nu(\mathrm{v})$ is the frequency of collisions, $\mu(\mathrm{v})\nu(\mathrm{v})$ is the probability of UCN losses, λ is the mean free path, and the relation $\lambda = 4V/S$ holds for an isotropic and homogeneous particle population in a trap of volume V and surface area S. Formula (18) shows that the inverse storage time is a linear function of inverse mean free path. The extrapolation of τ_{st}^{-1} to 0 frequency of collisions will give the probability of neutron β decay.

Unfortunately, correct extrapolation is impossible for the case of a wide UCN spectrum, which changes its form during the storage process owing to the velocity dependence of $\mu(\mathrm{v})$ and $\nu(\mathrm{v})$. To reduce the influence of this spectral dependence, Ref. [13] proposed fixing the number of collisions for different trap sizes by a suitable choice of the UCN holding time. This leads to the scaling relations

$$\frac{t_2(i)}{t_2(j)} = \frac{t_1(i)}{t_1(j)} = \frac{\lambda(i)}{\lambda(j)} = \frac{t_2(i) - t_1(i)}{t_2(j) - t_1(j)}, \qquad (19)$$

where t_1 and t_2 are two different UCN holding times used to determine τ_{st}^{-1}, and the indices (i, j) correspond to different volumes. Unfortunately, even when the scaling conditions are fulfilled, the extrapolation is faked owing to the gravitational field. The corresponding calculated correction is included in Ref. [13].

Quasielastic scattering of UCNs on the surface of liquid Fomblin changes the UCN spectrum and therefore also must be taken into account separately. A similar problem arises owing to above-barrier neutrons. In this article we demonstrate the importance of this additional correction, which was not taken into account in Ref. [13].

B. Monte Carlo simulation of the experiment in Ref. [13]

The relative importance of a particular effect (above-barrier neutrons or quasielastic scattering) to the final result can be investigated by switching it off in the simulation. Lacking knowledge of the temperature at which the experiment in Ref. [13] was carried out, we have performed our full analysis at 10°C, for which an analytical description of the model for quasielastic scattering of UCNs is given in Ref. [30].

Calculations were done on computing clusters, lasting about several months in total. In the following all detailed results are given for a reference volume with length $x = 55$ cm (see previous section) unless stated otherwise. Neutron reflection by the corrugated surface was approximated by 50% specular and 50% diffuse reflections from flat walls, if not stated differently. The time intervals of UCN holding were chosen as in the experiment. In all our simulations neutron lifetime was fixed at a definite value. Calculated corrections to the neutron lifetime extrapolated from our MC simulation were found to depend only weakly on the value chosen for τ_n.

Figure 7 shows, for illustration, some simulated data in comparison with experimental data. It demonstrates that our model shows a dependence similar to that in the experimental. Figure 2 in Ref. [13] shows typical behavior only, without specified experimental conditions (e.g., the surface structure of the movable wall). Without detailed experimental information we cannot reach full agreement with Fig. 2 in Ref. [13]. It should be explained that the most important results are the extrapolated neutron lifetime values. Therefore it is more correct to compare the behavior of the extrapolated τ_n as a function of holding time intervals.

Figure 8 is shown as a benchmark test of the extrapolated τ_n. One can see that we can reproduce the behavior of the extrapolated τ_n from holding time intervals for different types of surface of the movable wall owing to changes in specular reflectivity. The majority of the measurements in Ref. [13] were carried out with a corrugated surface because, in Table I there, just these data are shown. In our future analysis we will use 50% specular and 50% diffuse reflections, which describe the corrugated surface of the movable wall reasonably well.

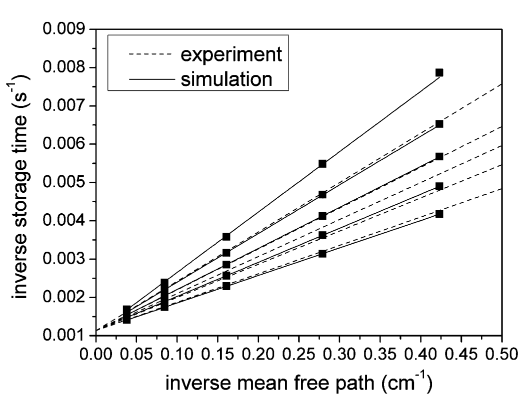

FIG. 7. Measured inverse bottle lifetimes as a function of the bottle inverse mean free path and for different holding intervals (dotted lines). Experimental data stem from Ref. [13]; they were quoted there as being typical. Results of simulation are shown by solid lines.

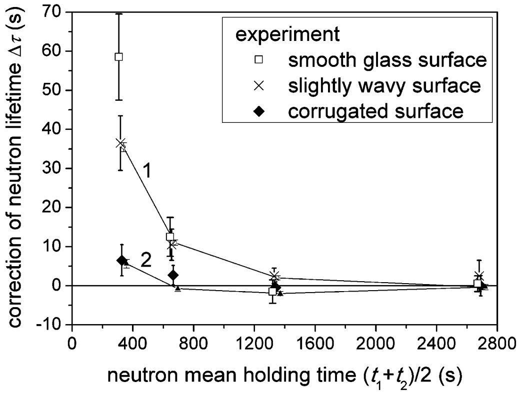

FIG. 8. Dependence of the uncorrected experimental neutron lifetime on holding time intervals for different bottle surface structures in comparison with results of simulations with different probabilities of specular reflections from the walls: (1) with 99% specular and 1% diffuse reflections; (2) with 50% specular and 50% diffuse reflections.

Next we investigated the dependence of simulation results on the initial UCN spectrum, which experimentally was known only poorly. Figure 9 demonstrates that this dependence is rather weak, particularly for the most important points with a long holding time (except for the low holding time, which at any rate had a negligible statistical weight in the result presented in Ref. [13]; see also Table III here). The corrections at the short holding time are proportional to the amplitude of the spectrum at a critical energy of 108 neV. In our future calculations we will use spectrum 4, shown by solid line in Fig. 9.

The effect of the spectral changes during the storage process is shown in Fig. 10. One can see that quasielastic scattering changes the form of the UCN spectrum considerably. Such changes are important, as they can cause a systematic error. Above-barrier neutrons can be stored for a long time, particularly if the energy is near the critical one.

The results of extrapolations to neutron lifetime are shown in Fig. 11 for different settings of the simulation including or excluding different effects. Excluding above-barrier neutrons and quasielastic scattering (curve 1), we can study the gravitational correction separately. Larger volumes have a larger relative area of the bottom plate and hence more UCN collisions with higher energy owing to gravity, resulting in lower values of extrapolated neutron lifetime. The gravitational correction is practically independent of the UCN holding time.

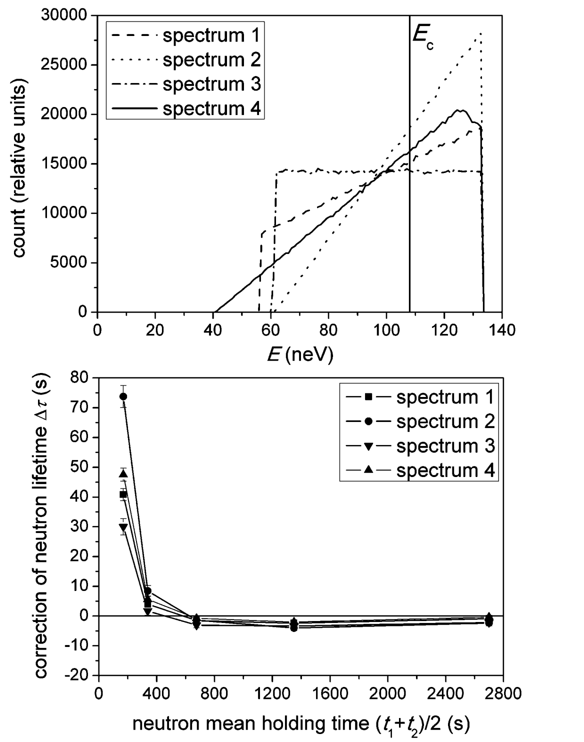

FIG. 9. Results of simulations with different initial UCN spectra in the trap. E_c is the critical energy of Fomblin oil (108 neV).

The extrapolated neutron lifetime is found to be lower than the neutron lifetime by 7.5 ± 0.3 s. This result is similar to the gravitational correction introduced in Ref. [13].

The next simulation shown in Fig. 11 was done including above-barrier neutrons in the UCN spectrum but without quasielastic scattering (curve 2). One can see that for a short holding time the extrapolated neutron lifetime is much higher in comparison with the previous case for the gravitational correction (curve 1), but for a long holding time the extrapolated neutron lifetime comes rather close to it. However, note, again, that the contribution of results with a short holding time in the final result in Ref. [13] is very small because of the poor statistical accuracy of these measurements. The points with a holding time of 900–1800 s and 1800–3600 s make the main contribution.

The next simulation shown in Fig. 11 was done taking into account quasielastic scattering but without above-barrier

TABLE III. Results for neutron lifetime τ_n obtained from different holding intervals: τ_n is the result from Ref. [13], $\Delta\tau$ [13] is the correction from Ref. [13], $\Delta\tau$ (this article) is the correction owing to above-barrier neutrons and quasielastic scattering calculated in this work, and $\tau_n' = \tau_n$(corrected [13]) + $\Delta\tau$(this article).

Holding interval (s)	τ_n(s): uncorrected [13]	$\Delta\tau$ (s): [13]	τ_n (s): corrected [13]	$\Delta\tau$ (s): this article	τ_n' (s)
112.5−225	893(10)	∼−2	891(10)		
225−450	885.0(4)	+3.5	888.5(4)		
450−900	881.2(2.5)	+8	889.2(2.5)	−7.84(0.87)	881.36(2.65)
900−1800	878.0(1.5)	+9	887.0(1.5)	−5.29(0.70)	881.71(1.65)
1800−3600	878.5(2.6)	+8.6	887.1(2.6)	−5.54(0.87)	881.56(2.74)
			τ_n = 887.6(1.1) s		τ_n' = 881.6(1.2) s

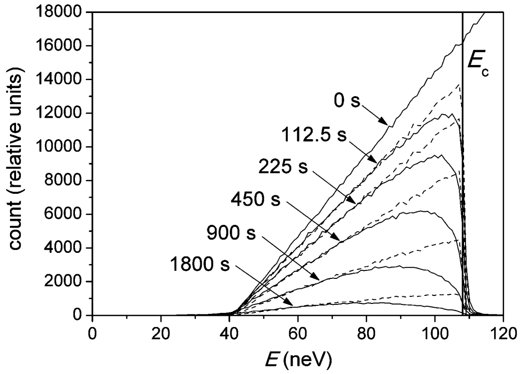

FIG. 10. UCN spectra in the trap after different holding intervals not taking quasielastic scattering into account (dotted lines) and taking quasielastic scattering into account (solid lines). E_c is the critical energy of Fomblin oil (108 neV).

neutrons (curve 4). One can see that with increasing holding time, the extrapolated τ_n increases owing to the appearance of new above-barrier neutrons.

The next simulation in Fig. 11 was done taking into account quasielastic scattering and above-barrier neutrons (curve 3). One can see that, owing to the appearance of new above-barrier neutrons from quasielastic scattering, the

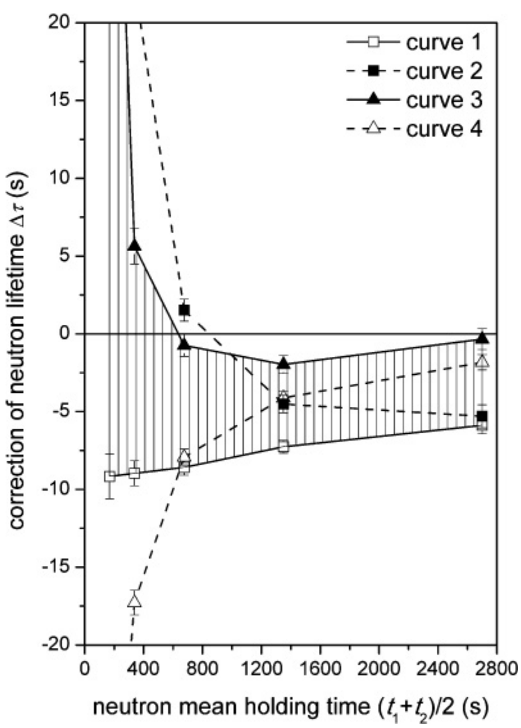

FIG. 11. Results of MC simulations of the extrapolated neutron lifetime for different holding intervals: (1) without quasielastic scattering and without above-barrier neutrons; (2) without quasielastic scattering and with above-barrier neutrons; (3) with quasielastic scattering and with above-barrier neutrons; (4) with quasielastic scattering and without above-barrier neutrons. The difference between curve 1 and curve 3 provides the correction owing to above-barrier neutrons and quasielastic scattering, which was not taken into account in Ref. [13].

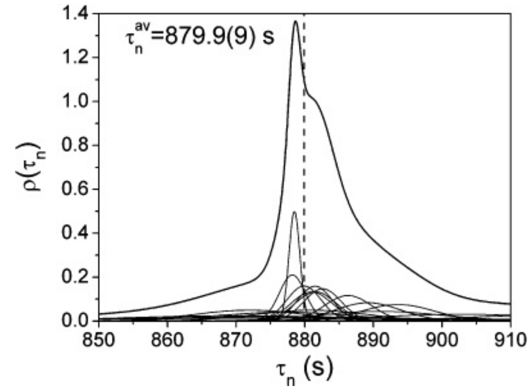

FIG. 12. Distribution of results of measurements of neutron lifetime after corrections and additions, giving the average value of 879.9 ± 0.9 s.

extrapolated τ_n cannot reach curve 1 at the long holding times. As a result, curve 3 is independent of the long holding times. This independence was interpreted in Ref. [13] as meaning that the process of cleaning of above-barrier neutrons is finished and the τ_n extrapolated to long holding times can be accepted as the correct value. Unfortunately, this is not true, owing to the effect of quasielastic scattering.

The difference between curve 1 and curve 3 is the total effect owing to above-barrier neutrons and quasielastic scattering. These effects were not taken into account in Ref. [13]. In Ref. [13] two corrections were introduced: a gravitational correction (+0.6%) and a correction connected with the small differences in the initial spectra depending on the bottle size (+0.3%). Table III quotes data from Ref. [13] with our additional corrections wing to above-barrier neutrons and quasielastic scattering effects. In this table we use the data for long holding time intervals, which make the main contribution and do not depend on entry conditions (form

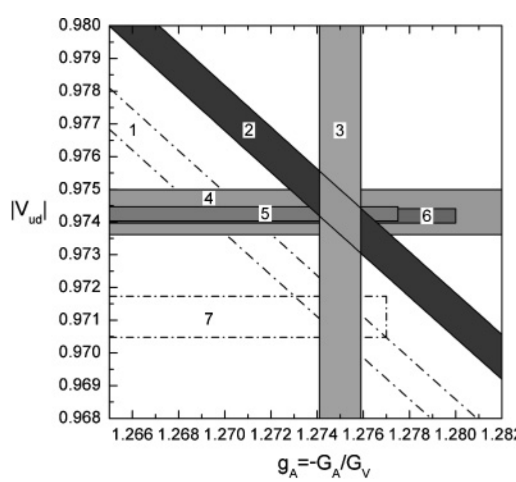

FIG. 13. Dependence of the CKM matrix element $|V_{ud}|$ on the values of the neutron lifetime and the axial coupling constant g_A. (1) Neutron lifetime (PDG 2006); (2) neutron lifetime (this article); (3) neutron β asymmetry (Perkeo 2007); (4) neutron β decay (this article + Perkeo 2007); (5) unitarity; (6) $0^+ \rightarrow 0^+$ nuclear transitions; (7) neutron β decay (PDG 2006 + Perkeo 2007).

of the initial spectrum, diffusion of a covering). As the total correction we find -6.0 ± 1.6 s. Our correction is a negative one and roughly compensates corrections from Ref. [13]. The systematic uncertainty in Ref. [13] is estimated as about 3 s. It can substantially cover for the lack of information on experiment details. The resulting corrected value for neutron lifetime would agree with the result 878.5 ± 0.8 s in Ref. [1].

IV. CONCLUSION

We provide a new table of results of neutron lifetime measurements taking into account the correction of Refs. [6] and [7] and, also, Refs. [13] and [14]. We also include in the table the result of the MAMBO II experiment [8] based on MAMBO I. It uses a UCN spectrum with a cutoff below the Fomblin critical energy. Because of this the systematic error of the MAMBO I experiment is suppressed. Reference [11] can be withdrawn from the list, as a new, much more accurate result has been obtained with this installation using low-temperature Fomblin rather than solid oxygen. The difference between the earlier result and the new one is 2.9 standard deviations. It is reasonable to withdraw the previous result owing to obtaining the new, more accurate result. Finally, it is necessary to include the new result of Morozov's group [3]. Then after corrections and additions, the table of experimental results for neutron lifetime looks as shown here (Table I, Fig. 12). The standard error of the average value from Table I is 0.6 s, but the standard deviation of experimental results is 0.9 s. Thus, it will be expedient to accept 879.9 ± 0.9 s as the world average value for neutron lifetime.

Finally, we must mention that analysis of neutron β decay with the new world average neutron lifetime demonstrates reasonable agreement in the frame of the standard model. Figure 13 shows this analysis, which is discussed in detail in Refs. [31] and [32]. Figure 13 shows the dependence of the CKM matrix element on the values of the neutron lifetime and the axial coupling constant g_A. The value $|V_{\mathrm{ud}}| = 0.9743(7)$, calculated for the new world average value for neutron lifetime of 879.9(9) s and $g_A = 1.2750(9)$ [33], agrees with both $|V_{\mathrm{ud}}| = 0.97419(22)$ from the unitarity of the CKM matrix elements [2] and $|V_{\mathrm{ud}}| = 0.97425(22)$, measured from the superallowed $0^+ \to 0^+$ nuclear β decays, caused by pure Fermi transitions only [33,34].

One can see that the value $|V_{\mathrm{ud}}| = 0.9711(6)$, calculated for the old world average value for neutron lifetime of 885.7(8) s, is ruled out by the experimental values $|V_{\mathrm{ud}}| = 0.97419(22)$ and $|V_{\mathrm{ud}}| = 0.97425(22)$.

In addition, it should be mentioned that a detailed analysis of the nucleosynthesis process in the early stages of the formation of the Universe has been made [35]. Those authors analyzed the effect of the new value of the neutron lifetime on the consistency of data on the initial abundances of D and ^{4}He isotopes and data on baryon asymmetry η_{10}. The use of the new value of the neutron lifetime improves the agreement between the data on the initial abundances of deuterium and helium and the data on baryon asymmetry. Although the accuracy of the cosmological data is much lower than that of measurements of the neutron lifetime, the shift of τ_{n} from the world average value to the new value has a certain effect on the verification of the nucleosynthesis model in the early stages of the formation of the Universe.

ACKNOWLEDGMENTS

The authors are grateful to V. I. Morozov and L. N. Bondarenko for providing the information on the geometry of the experimental setup and critical remarks. We would like to pay great tribute to the main initiator of the experiment in Ref. [13], Walter Mampe, who made a very significant contribution to the development of UCN experiments at ILL and who succeeded in uniting physicists from different countries to carry out these tasks. We are very grateful to Mike Pendlebury for useful discussions in the course of this work. We also would like to thank Oliver Zimmer for critical remarks on the manuscript. Calculations were done at the PNPI ITAD computing cluster and PNPI PC Farm. The investigation was supported by Russian Foundation for Basic Research Project Nos. 07–02-00859-a, 08–02-01052-a, 10–02-00217-a, and 10–02-00224-a. The work was also supported by the Federal Agency of Education, under state contract nos. P2427, P2500, and P2540. In addition, it was supported by the Federal Agency of Science and Innovations, under state Contract No. 02.740.11.0532.

[1] A. Serebrov *et al.*, Phys. Lett. B **605**, 72 (2005); A. P. Serebrov *et al.*, Phys. Rev. C **78**, 035505 (2008).
[2] C. Amsler *et al.* (Particle Data Group), Phys. Lett. B **667**, 1 (2008); 2009 partial update for the 2010 edition [http://pdg.lbl.gov].
[3] P. Geltenbort, in *Proceedings of The Seventh UCN Workshop, St. Petersburg, Russia* (2009); [http://cns.pnpi.spb.ru/ucn/articles/Geltenbort.pdf].
[4] V. Ezhov, in *Proceedings of The Seventh UCN Workshop, St. Petersburg, Russia* (2009); [http://cns.pnpi.spb.ru/ucn/articles/Ezhov1.pdf].
[5] M. S. Dewey *et al.*, Phys. Rev. Lett. **91**, 152302 (2003).
[6] S. Arzumanov *et al.*, Phys. Lett. B **483**, 15 (2000).
[7] A. K. Fomin and A. P. Serebrov, Pis'ma Zh. Eksp. Teor. Fiz. **92**, 16 (2010); JETP Lett. **92**, 40 (2010) [http://jetpletters.ac.ru/ps/1902/article_28888.shtml].
[8] A. Pichlmaier *et al.*, Nucl. Instrum. Methods A **440**, 517 (2000).
[9] J. Byrne *et al.*, Europhys. Lett. **33**, 187 (1996).
[10] W. Mampe *et al.*, Pis'ma Zh. Eksp. Teor. Fiz. **57**, 77 (1993) [http://jetpletters.ac.ru/ps/284/article_4588.shtml]; JETP Lett. **57**, 82 (1993) [http://jetpletters.ac.ru/ps/1175/article_17737.shtml].
[11] V. V. Nesvizhevskii *et al.*, Zh. Eksp. Teor. Fiz. **102**, 740 (1992) [http://www.jetp.ac.ru/cgi-bin/e/index/r/102/3/p740?a=list]; JETP **75**, 405 (1992) [http://www.jetp.ac.ru/cgi-bin/e/index/e/75/3/p405?a=list].

[12] J. Byrne *et al.*, Phys. Rev. Lett. **65**, 289 (1990).

[13] W. Mampe, P. Ageron, C. Bates, J. M. Pendlebury, and A. Steyerl, Phys. Rev. Lett. **63**, 593 (1989).

[14] A. P. Serebrov and A. K. Fomin, Pis'ma Zh. Eksp. Teor. Fiz. **90**, 607 (2009); JETP Lett. **90**, 555 (2009) [http://jetpletters.ac.ru/ps/1880/article_28640.shtml].

[15] A. G. Kharitonov *et al.*, Nucl. Instrum. Methods A **284**, 98 (1989).

[16] R. Kossakowski *et al.*, Nucl. Phys. A **503**, 473 (1989).

[17] W. Paul *et al.*, Z. Phys. C **45**, 25 (1989).

[18] P. E. Spivak, Zh. Eksp. Teor. Fiz. **94**, 1 (1988) [http://www.jetp.ac.ru/cgi-bin/e/index/r/94/9/p1?a=list]; JETP **67**, 1735 (1988) [http://www.jetp.ac.ru/cgi-bin/e/index/e/67/9/p1735?a=list].

[19] J. Last, M. Arnold, J. Dohner, D. Dubbers, and S. J. Freedman, Phys. Rev. Lett. **60**, 995 (1988).

[20] M. Arnold, Dissertation, University of Heidelberg, 1987.

[21] Yu. Yu. Kosvintsev *et al.*, Pis'ma Zh. Eksp. Teor. Fiz. **44**, 444 (1986) [http://jetpletters.ac.ru/ps/152/article_2623.shtml]; JETP Lett. **44**, 571 (1986) [http://jetpletters.ac.ru/ps/1397/article_21182.shtml].

[22] J. Byrne *et al.*, Phys. Lett. B **92**, 274 (1980).

[23] L. N. Bondarenko *et al.*, Pis'ma Zh. Eksp. Teor. Fiz. **28**, 329 (1978) [http://jetpletters.ac.ru/ps/501/article_7926.shtml]; JETP Lett. **28**, 303 (1978) [http://jetpletters.ac.ru/ps/1575/article_24154.shtml].

[24] C. J. Christensen *et al.*, Phys. Rev. D **5**, 1628 (1972).

[25] A. K. Fomin, Ph.D. thesis, PNPI, Gatchina, 2006.

[26] F. Atchison *et al.*, Nucl. Instrum. Methods Phys. Res. A **552**, 513 (2005).

[27] A. I. Fomin, in *Proceedings of The First UCN Workshop, Pushkin, Russia* (1998).

[28] A. I. Fomin, Ph.D. thesis, Kurchatov Institute, Moscow, 2000.

[29] I. K. Kikoin, ed., *Tables of Physical Values, Directory* (Atomisdat, Moscow, 1976) (in Russian).

[30] S. K. Lamoreaux and R. Golub, Phys. Rev. C **66**, 044309 (2002).

[31] A. P. Serebrov, Phys. Lett. B **650**, 321 (2007).

[32] M. Faber *et al.*, Phys. Rev. C **80**, 035503 (2009).

[33] H. Abele, Prog. Part. Nucl. Phys. **60**, 1 (2008).

[34] J. C. Hardy and I. S. Towner, Phys. Rev. C **79**, 055502 (2009).

[35] G. J. Mathews, T. Kajino, and T. Shima, Phys. Rev. D **71**, 021302(R) (2005).